Radiative corrections to electronpion scattering revisited

N Kaiser

Radiative corrections to electron-pion scattering revisited

N. Kaiser

Physik-Department T39, Technische Universität München, D-85747 Garching, Germany

Abstract

We calculate in closed analytical form the one-loop radiative corrections to electron-pion scattering $e^-\pi^- \to e^-\pi^-$. Concise expressions (in terms of dimensionless Mandelstam variables) are given for the pertinent interference terms between the tree diagram and the one-loop diagrams related to photonic vertex correction, vacuum polarization and two-photon exchange. Infrared finiteness of these virtual radiative corrections is achieved (in the standard way) by including soft photon radiation below an energy cut-off λ. We evaluate the finite part of the soft photon correction factor in the center-of-mass frame. For all contributions we keep the full dependence on the electron mass. The results for the loop amplitudes can be applied also to pion-pair production $e^-e^+ \to \pi^+\pi^-$. The radiative corrections to the corresponding total cross section are calculated with consideration of the pion-structure via a vector meson dominance form factor. We find that such an additional charge form factor (inserted into the photonic vertex correction of the pion) changes the radiative corrections to the total cross section by about -0.2%.

PACS: 12.20.-m, 12.20.Ds, 14.70.Bh

1 Introduction and summary

For a correct interpretation of the experimental data obtained in elastic or inelastic lepton scattering processes it is essential to include in the analysis of these data the radiative corrections arising from virtual photon-loops and (soft) photon bremsstrahlung. The subject of radiative corrections has by now already a long history and we refer to the standard review papers of Maximon [1] and Mo and Tsai [2] which have been used in the interpretation of many electron scattering experiments. In recent years the issue of radiative corrections has received a renewed interest in connection with new precision experiments, performed e.g. at JLAB or MAMI. The two-photon exchange contribution [3, 4, 5] to the elastic electron-proton scattering plays in fact a crucial role in order to reconcile the apparent discrepancies for the ratio of the proton electric and magnetic form factors $G_E^p(Q^2)/G_M^p(Q^2)$ as determined with the polarization transfer technique on the one hand side and via the (more traditional) Rosenbluth separation method on the other hand side.

These findings have prompted the exploration of the significance of two-photon exchange in other electromagnetic reactions (see ref.[6] for a recent review on this subject). In particular, the two-photon exchange corrections to elastic electron-pion scattering have been calculated in ref.[7] taking into account the finite size of the pion through a (phenomenological) monopole form factor $F_\pi(Q^2) = (1 + Q^2/m_\rho^2)^{-1}$. It has been found, that in comparison to the soft-photon approximation which neglects hadron structure effects, the corrections are less than 1% for low momentum transfers $Q^2 < 0.1\,\mathrm{GeV}^2$, but can increase to several percent for $Q^2 \geq 1\,\mathrm{GeV}^2$ at extreme backward angles. The analytical expression for the two-photon exchange amplitude with insertion of monopole form factors at the photon-pion vertices has however

not been provided in ref.[7]. Also the two-photon exchange diagram involving the two-photon-pion contact-vertex has seemingly been omitted, although the pion Compton tensor becomes transversal only after that contact-vertex is properly included. Presumably its effect is so small that it does not change the numerical results of ref.[7] in a significant way.

The one-loop radiative corrections to elastic electron-pion scattering $e^-\pi^- \to e^-\pi^-$ have calculated some time ago by Kahane in ref.[8]. The associated inelastic bremsstrahlung process $e^-\pi^- \to e^-\pi^-\gamma$ including soft photons (to cancel the infrared divergences generated by the photon-loops) as well as hard photons has also been considered in detail and in the end the radiative corrections have been approximated by their dominant logarithmic terms. Unfortunately, the comprehensibility of the various analytical formulas written in ref.[8] is not always straightforward since lots of auxiliary variables have been introduced although the process $e^-\pi^- \to e^-\pi^-$ can be described by just two independent Mandelstam variables.

In this situation it is still meaningful and helpful to reconsider the radiative corrections to electron-pion scattering. The purpose of the present paper is to document the results of such a careful rederivation. Our paper is organized as follows. In section 2, we calculate in closed analytical form the one-loop radiative corrections to electron-pion scattering $e^-\pi^- \to e^-\pi^-$, treating the pion as a structureless spin-0 particle. Explicit expressions (in terms of suitable dimensionless Mandelstam variables) are given for the pertinent interference terms between the tree diagram and the one-loop diagrams averaged already over the electron spin-states. The occurring one-loop diagrams are of the type: photonic vertex correction, vacuum polarization and two-photon exchange. Infrared finiteness of these virtual radiative corrections is achieved (in the standard way) by including soft photon radiation (off the in- or out-going charged particles) below an energy cut-off λ. We evaluate the remaining finite part of the soft photon correction factor in the center-of-mass frame, assuming an isotropic photon emission therein. In contrast to most existing calculations of the radiative corrections we keep in all expressions the full dependence on the electron mass m_e. This has the advantage that our analytical results can be directly taken over to muon-pion scattering where the knowledge of the complete dependence on the lepton mass m_μ is necessary. Figures with numerical results are presented in order to demonstrate the size as well as the energy and angular dependence of the radiative corrections to electron-pion scattering in the low-energy region. The radiative corrections are dominated by the electronic vertex correction and the two-photon exchange. By making use of crossing symmetry the radiative corrections to pion-pair production $e^-e^+ \to \pi^+\pi^-$ can be obtained from the same analytical formulas. As a special feature, the contributions from two-photon exchange drop out in the (angle-integrated) total cross section. We calculate in section 3, the radiative corrections to $\sigma_{\rm tot}(e^-e^+ \to \pi^+\pi^-)$ taking into account the pion-structure through a charge form factor of monopole type. The relevant photon-loop including a squared monopole form factor can be evaluated neatly with the help of a (once-subtracted) dispersion relation. In this (semi-phenomenological) approach we find that the pion-structure changes the radiative corrections to the total cross section $\sigma_{\rm tot}(e^-e^+ \to \pi^+\pi^-)$ by about -0.2%. Another important effect that must be included is the hadronic vacuum polarization for which (continuously improving) parameterizations are available (see for that purpose the discussion in section 6 of ref.[9]).

The results of this work can be of some relevance for extracting with improved precision the hadronic cross section $\sigma_{\rm tot}(e^-e^+ \to \pi^+\pi^-)$ which presently causes the largest part of the errorbar for the hadronic vacuum polarization contribution [9] to the muon anomalous magnetic moment. An accurate knowledge of the electromagnetic interaction of pions is obviously a crucial condition for that procedure.

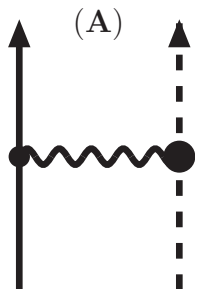

Figure 1: One-photon exchange tree diagram (A) for electron-pion scattering. Full, dashed and wiggly lines denote electrons, pions and photons, respectively.

2 Radiative corrections to electron-pion scattering

We start out with calculating the radiative corrections to electron-pion scattering. The in- and out-going four-momenta of the reaction $e^-(p_1) + \pi^-(p_2) \to e^-(p_3) + \pi^-(p_4)$ give rise to the Lorentz-invariant (dimensionless) Mandelstam variables (s, t, u) defined as follows:

$$s\, m_\pi^2 = (p_1 + p_2)^2\,, \qquad t\, m_\pi^2 = (p_1 - p_3)^2\,, \qquad u\, m_\pi^2 = (p_1 - p_4)^2\,. \tag{1}$$

Since m_π^2 has been factored out, they obey the numerical constraint $s + t + u = 2 + 2r$ with $r = (m_e/m_\pi)^2$ the squared ratio between the electron mass $m_e = 0.511\,\text{MeV}$ and the pion mass $m_\pi = 139.57\,\text{MeV}$. In the case of unpolarized scattering the squared T-matrix for $e^-\pi^- \to e^-\pi^-$ has to be summed over the electron spin-states. This double sum is efficiently performed via a Dirac-trace: $\frac{1}{8}\text{tr}[O(\not{p}_1 + m_e)\overline{O}(\not{p}_3 + m_e)]$. In order to keep the technical complication of the loop calculation as low as possible the integration over the loop-momenta is carried out after the summation over the electron spin-states. With that approach in mind the unpolarized differential cross section for electron-pion scattering in the center-of-mass frame, including radiative corrections of relative order α, can be represented in the following compact form:

$$\frac{d\sigma}{d\Omega_{\text{cm}}} = \frac{\alpha^2}{m_\pi^2 s}\left\{\frac{A\otimes A}{t^2} + \frac{2}{t}\,\text{Re}\Big[(\text{I} + \text{II} + \text{III} + \text{IV} + \text{V})\otimes A\Big]\right\}, \tag{2}$$

with $\alpha = 1/137.036$ the fine-structure constant. Here A denotes the one-photon exchange tree diagram (shown in Fig. 1) and I, II, III, IV, V stand for the five (classes of) contributing one-loop diagrams (shown in Figs. 2, 3, 4). The product symbol $\otimes$ designates the interference term between the T-matrices from two diagrams with the sums over the electron spins already carried out via a Dirac-trace. When written in terms of the dimensionless variables (s, t, u, r) the tree diagram A in Fig. 1 leads to the following simple polynomial expression:

$$A\otimes A = 1 - (s - r)(u - r)\,. \tag{3}$$

Note the invariance of $A\otimes A$ under the crossing transformation $s \leftrightarrow u$. It expresses the obvious fact that at leading order the differential cross sections for $e^-\pi^- \to e^-\pi^-$ and $e^-\pi^+ \to e^-\pi^+$ are equal.

2.1 Evaluation of one-loop diagrams

In this section, we present analytical expressions (of order α) for the interference terms between the tree diagram and the one-loop diagrams for electron-pion scattering. We use dimensional

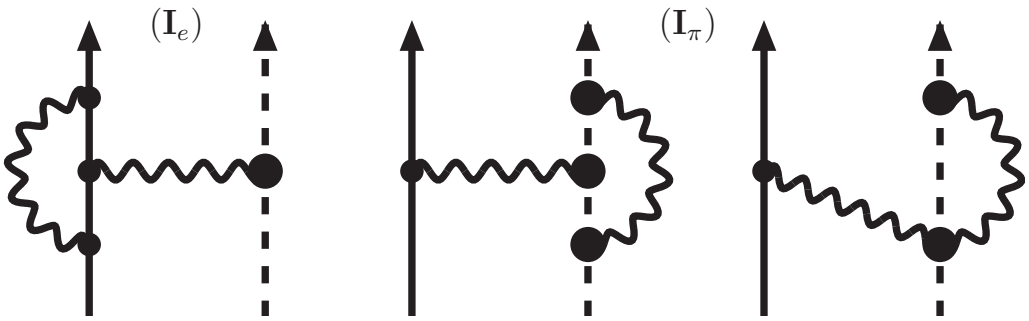

Figure 2: One-loop diagrams (I) with photonic vertex corrections. The right diagram has a horizontally reflected partner.

regularization to treat both ultraviolet and infrared divergences (where the latter are caused by the masslessness of the photon). Divergent pieces of one-loop integrals show up in form of the composite constant:

$$\xi = \frac{1}{d-4} + \frac{1}{2}(\gamma_E - \ln 4\pi) + \ln\frac{m_e}{\mu}\,, \tag{4}$$

containing a simple pole at $d = 4$ and μ is an arbitrary mass scale. Ultraviolet (UV) and infrared (IR) divergences are distinguished by the feature of whether the condition for convergence of the d-dimensional integral is $d < 4$ or $d > 4$. We discriminate them in the notation by putting appropriate subscripts, i.e. ξ_{UV} and ξ_{IR}.[1] In order to simplify all calculations, we employ the Feynman gauge where the photon propagator is directly proportional to the Minkowski metric tensor $g^{\mu\nu}$. Let us now enumerate the analytical results as they emerge from the five (classes of) one-loop diagrams shown in Figs. 2, 3, 4.

The (on-shell) vertex correction in diagram I_e is comprised by the one-photon loop form factors $F_{1,2}(t)^{\gamma-\mathrm{loop}}$ of the electron. These Dirac and Pauli form factors are normalized at $t = 0$ to: $F_1(0)^{\gamma-\mathrm{loop}} = 0$ and $F_2(0)^{\gamma-\mathrm{loop}} = \alpha/2\pi$ (anomalous magnetic moment). Putting all the pieces together the pertinent interference term $(A \otimes A)F_1(t)^{\gamma-\mathrm{loop}}/t + (1 - t/4)F_2(t)^{\gamma-\mathrm{loop}}$ with the tree diagram A reads:

$$\begin{aligned}\mathrm{I}_e \otimes A \;=\; & \frac{\alpha}{2\pi t}\Bigg\{\Bigg[\Big(4\xi_{IR}(t-2r) + 8r - 3t\Big)\frac{L(-tr^{-1})}{\sqrt{4r^2 - rt}} + 2\xi_{IR} - 2 \\ & + \frac{(t-2r)\Phi(-tr^{-1})}{\sqrt{-t}\sqrt{4r-t}}\Bigg](A \otimes A) + \sqrt{r}(4t - t^2)\frac{L(-tr^{-1})}{\sqrt{4r-t}}\Bigg\}\,,\end{aligned} \tag{5}$$

with $A \otimes A$ given in eq.(3). Here, we have introduced the frequently occurring logarithmic loop function:

$$L(x) = \frac{1}{\sqrt{x}}\ln\frac{\sqrt{4+x} + \sqrt{x}}{2}\,, \tag{6}$$

and the auxiliary function:

$$\Phi(x) = \mathrm{Li}_2(v(x)) - \mathrm{Li}_2(1 - v(x)) + \frac{1}{2}\ln^2 v(x) - \frac{1}{2}\ln^2(1 - v(x))\,, \tag{7}$$

composed of dilogarithms and squared logarithms of the argument:

$$v(x) = \frac{1}{2}\Big(1 - \sqrt{\frac{x}{4+x}}\Big)\,, \tag{8}$$

[1] If an infinitesimal photon mass m_γ is introduced as an (alternative) infrared regulator the infrared divergence ξ_{IR} is to be identified with the logarithm $\ln(m_e/m_\gamma)$.

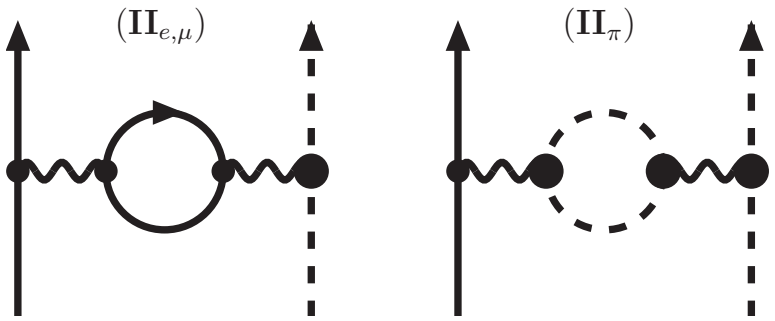

Figure 3: One-loop diagrams (II) with leptonic or pionic vacuum polarizations.

where $\mathrm{Li}_2(v) = \sum_{n=1}^{\infty} n^{-2} v^n = v \int_1^{\infty} dy [y(y-v)]^{-1} \ln y$ denotes the conventional dilogarithmic function. The basic loop function $\Phi(-t)/(\sqrt{-t}\sqrt{4-t})$ possesses the following spectral representation:

$$\frac{\Phi(-t)}{\sqrt{-t}\sqrt{4-t}} = \int_4^{\infty} \frac{dx}{x-t} \frac{\ln(x-4)}{\sqrt{x^2-4x}}\,. \tag{9}$$

Note that in addition to the photon-loop also the counterterm $Z_1^{(e)} - 1 = \alpha(2\xi_{IR} + \xi_{UV} - 2)/2\pi$ of spinor quantum electrodynamics, which eliminates the ultraviolet divergence ξ_{UV} in the Dirac form factor $F_1(t)^{\gamma-\mathrm{loop}}$, has been included in eq.(5).

In the same way, the (on-shell) vertex corrections in diagrams I_π are comprised by the one-photon loop form factor $G_\pi(t)^{\gamma-\mathrm{loop}}$ of the pion. When completed by the counterterm contribution $Z_1^{(\pi)} - 1 = \alpha(\xi_{IR} - \xi_{UV})/\pi$ of scalar quantum electrodynamics this form factor is also normalized to $G_\pi(0)^{\gamma-\mathrm{loop}} = 0$. The pertinent interference term $(A \otimes A) G_\pi(t)^{\gamma-\mathrm{loop}}/t$ with the tree diagram reads:

$$\begin{aligned} \mathrm{I}_\pi \otimes A \;\; = \;\; & \frac{\alpha}{2\pi t}\Big\{ 2\xi_{IR} - 2 - \ln r + \frac{t-2}{\sqrt{-t}\sqrt{4-t}}\Big[\Phi(-t) \\ & + (4\xi_{IR} - 4 - 2\ln r)\sqrt{-t}\, L(-t)\Big]\Big\}(A \otimes A)\,. \end{aligned} \tag{10}$$

The additional $\ln r$ terms are present because the infrared divergence ξ_{IR} has been defined in eq.(4) with the electron mass in the logarithm $\ln(m_e/\mu)$.

The diagrams of class II shown in Fig. 3 involve vacuum polarizations at the exchanged photon. Together with the counterterm $Z_3^{(e)} - 1 = 2\alpha\, \xi_{UV}/3\pi$ the (renormalized) contribution from electronic vacuum polarization takes the form:

$$\mathrm{II}_e \otimes A = \frac{\alpha}{3\pi t^2}\Big\{ \frac{2}{\sqrt{r}}(t+2r)\sqrt{4r-t}\, L(-tr^{-1}) - \frac{5t}{3} - 4r \Big\}(A \otimes A)\,. \tag{11}$$

The analogous contribution from muonic vacuum polarization $\mathrm{II}_\mu \otimes A$ is readily obtained by replacing the parameter r in eq.(11) by $\tilde{r} = (m_\mu/m_\pi)^2 = 0.57309$. In addition there is the pionic vacuum polarization diagram II_π. Together with the tadpole diagram (generated by the $\gamma\gamma\pi\pi$ contact-vertex) and the counterterm $Z_3^{(\pi)} - 1 = \alpha(\xi_{UV} - \frac{1}{2}\ln r)/6\pi$ the complete (renormalized) contribution from pionic vacuum polarization reads:

$$\mathrm{II}_\pi \otimes A = \frac{\alpha}{6\pi t^2}\Big\{ 4 - \frac{4t}{3} + (t-4)\sqrt{4-t}\, L(-t) \Big\}(A \otimes A)\,. \tag{12}$$

Next, we come to the two-photon exchange triangle diagram III shown in Fig. 4. The respective loop integral with one massive (pion) and two massless (photon) propagators is

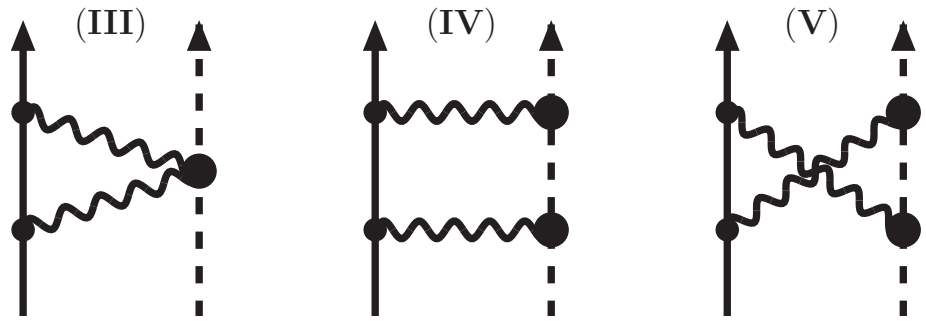

Figure 4: Two-photon exchange diagrams (III), (IV) and (V) for electron-pion scattering.

infrared convergent and the pertinent interference term with the tree diagram takes the form:

$$\mathrm{III} \otimes A = \frac{\alpha}{\pi}\frac{s-u}{4r-t}\Big\{(4r-2t)K(tr^{-1}) + r\Big[\ln r - \ln(-t)\Big]\Big\}\,, \tag{13}$$

with the t-dependent auxiliary function:

$$K(t) = \frac{1}{\sqrt{-t}\sqrt{4-t}}\Big[\frac{\pi^2}{3} - t\,L^2(-t) + \mathrm{Li}_2\Big(\frac{2-t-\sqrt{-t}\sqrt{4-t}}{2}\Big)\Big]\,. \tag{14}$$

Somewhat more intricate is the evaluation of the (planar and crossed) two-photon exchange box diagrams IV and V shown in Fig. 4. We take advantage of performing first the spin-sums (via a Dirac-trace) and of decomposing in the next step the resulting Lorentz-scalar loop integrand into partial fractions. In this form the majority of terms has either only one electron propagator or only one pion propagator and few terms involve the product of both. The latter loop integrals depend in a non-trivial way on the squared mass ratio $r = (m_e/m_\pi)^2$. Putting all the pieces together one finds for the interference term of the planar two-photon exchange box diagram IV with the following analytical expression:

$$\begin{aligned}
\mathrm{IV} \otimes A \;=\; & \frac{\alpha}{\pi}\Big\{\frac{s}{2}(s-2r)K(t) + \frac{s}{2r}(s-2-2r)K(tr^{-1}) \\
& + \frac{1+r-s}{\sqrt{\rho_+ - s}\sqrt{\rho_- - s}}\Big[(4\xi_{IR} - 2\ln r)\Big(s - r + \frac{1}{t}(s-1-r)^2\Big) \\
& + \Big(s - r + \frac{2}{t}(s-1-r)^2\Big)\ln(-t)\Big]\ln\frac{\sqrt{\rho_+ - s} + \sqrt{\rho_- - s}}{2r^{1/4}} \\
& + \frac{1}{2}(s-r)(1+r-s)\int_{\rho_+}^{\infty}\frac{dx}{x-s}\,\frac{\ln[x-2-2r+(1-r)^2x^{-1}]}{\sqrt{x^2-2x(1+r)+(1-r)^2}} \\
& + \text{terms even under } (s \leftrightarrow u)\Big\}\,,
\end{aligned} \tag{15}$$

with the abbreviations $\rho_\pm = 1 + r \pm 2\sqrt{r}$. For the numerical evaluation of the (only relevant) real part of IV$\otimes A$ the spectral integral $\int_{\rho_+}^{\infty} dx/(x-s)\ldots$ in the second last line of eq.(15) has to be treated as a principal value integral (if $s > \rho_+$). It can be conveniently decomposed into a sum of two non-singular integrals by the following master formula:

$$\fint_{\rho_+}^{\infty} dx\,\frac{f(x)}{x-s} = \int_{\rho_+}^{2s-\rho_+} dx\,\frac{f(x)-f(s)}{x-s} + \int_{2s-\rho_+}^{\infty} dx\,\frac{f(x)}{x-s}\,. \tag{16}$$

Finally, we are left with the contribution of the crossed two-photon exchange box diagram V shown in Fig. 4. Its interference term with the tree diagram can be obtained via crossing ($s \to u = 2 + 2r - s - t$) as follows:

$$\mathrm{V} \otimes A = -\,\mathrm{IV} \otimes A\,|_{s \leftrightarrow u}\,. \tag{17}$$

The occurring minus-sign has the consequence that all terms even under the permutation of variables $s \leftrightarrow u$ drop out in the sum $(\mathrm{IV} + \mathrm{V}) \otimes A$ and therefore we do not need to specify these. We have verified the relation eq.(17) by an explicit calculation of $\mathrm{V} \otimes A$ as it arises from the crossed two-photon exchange diagram V. The physical reason behind eq.(17) can be easily explained and understood. When turning the right pion line in the crossed two-photon exchange diagram V upside-down one gets the planar two-photon exchange diagram IV for electron-antipion scattering ($e^-\pi^+ \to e^-\pi^+$). The same manipulation applied to the tree diagram A introduces an additional minus sign due to the (single) opposite electric charge, and to close the argument, $e^-\pi^+ \to e^-\pi^+$ and $e^-\pi^- \to e^-\pi^-$ are connected with each other by $s \leftrightarrow u$ crossing.

As an aside we note that it is instrumental to keep the factorized square roots in eqs.(5,10-15) as they stand. In this form the correct analytical continuation of the (only relevant) real parts of the loop functions along their branch cuts is guaranteed.

2.2 Infrared finiteness

In the next step we have to consider the infrared divergent terms proportional to ξ_{IR}. Inspection of eqs.(5,10,15,17) reveals that these scale with the Born term $A \otimes A/t$. As a consequence of that feature, the infrared divergent loop corrections multiply the differential cross section $d\sigma/d\Omega_{\rm cm}$ at tree-level by a factor:

$$\begin{aligned}
\delta_{\rm virt}^{(IR)} &= \frac{4\alpha}{\pi}\xi_{IR}\Big\{1 + \frac{t-2}{\sqrt{4-t}}\,L(-t) + \frac{t-2r}{\sqrt{4r^2-rt}}\,L(-tr^{-1}) \\
&\quad + \mathrm{Re}\Big[\frac{2(1+r-s)}{\sqrt{\rho_+ - s}\sqrt{\rho_- - s}}\ln\frac{\sqrt{\rho_+ - s} + \sqrt{\rho_- - s}}{2r^{1/4}}\Big] \\
&\quad + \frac{2(u-1-r)}{\sqrt{\rho_+ - u}\sqrt{\rho_- - u}}\ln\frac{\sqrt{\rho_+ - u} + \sqrt{\rho_- - u}}{2r^{1/4}}\Big\}\,.
\end{aligned} \tag{18}$$

The unphysical infrared divergence ξ_{IR} gets removed in the measurable cross section by contributions from (undetected) soft photon bremsstrahlung. In its final effect, the (single) soft photon radiation off the in- or out-going electrons and pions yields the multiplicative factor:

$$\begin{aligned}
\delta_{\rm soft} &= \alpha\,\mu^{4-d}\int\limits_{|\vec{l}|<\lambda}\frac{d^{d-1}l}{(2\pi)^{d-2}\,l_0}\Big\{\frac{2p_1\cdot p_3}{p_1\cdot l\,p_3\cdot l} + \frac{2p_2\cdot p_4}{p_2\cdot l\,p_4\cdot l} + \frac{2p_1\cdot p_4}{p_1\cdot l\,p_4\cdot l} + \frac{2p_2\cdot p_3}{p_2\cdot l\,p_3\cdot l} \\
&\quad - \frac{2p_1\cdot p_2}{p_1\cdot l\,p_2\cdot l} - \frac{2p_3\cdot p_4}{p_3\cdot l\,p_4\cdot l} - \frac{m_e^2}{(p_1\cdot l)^2} - \frac{m_\pi^2}{(p_2\cdot l)^2} - \frac{m_e^2}{(p_3\cdot l)^2} - \frac{m_\pi^2}{(p_4\cdot l)^2}\Big\}\,,
\end{aligned} \tag{19}$$

which depends on a small photon energy cut-off λ. Working out this momentum space integral by the method of dimensional regularization (with $d > 4$) one obtains the following soft photon correction factor [11]:

$$\begin{aligned}
\delta_{\rm soft}^{(\rm cm)} &= \frac{\alpha}{\pi}\Big\{4\Big[1 + \frac{t-2}{\sqrt{4-t}}\,L(-t) + \frac{t-2r}{\sqrt{4r^2-rt}}\,L\Big(-\frac{t}{r}\Big)
\end{aligned}$$

$$
\begin{aligned}
&+\frac{2}{\sqrt{P}}(s-1-r)\ln\frac{\sqrt{s-\rho_+}+\sqrt{s-\rho_-}}{2r^{1/4}}\\
&+\frac{2(u-1-r)}{\sqrt{\rho_+-u}\sqrt{\rho_--u}}\ln\frac{\sqrt{\rho_+-u}+\sqrt{\rho_--u}}{2r^{1/4}}\Bigg]\left(\ln\frac{m_e}{2\lambda}-\xi_{IR}\right)+\frac{2}{\sqrt{P}}\\
&\times\left[(s-1+r)\ln\frac{s-1+r+\sqrt{P}}{2\sqrt{sr}}+(s+1-r)\ln\frac{s+1-r+\sqrt{P}}{2\sqrt{s}}\right]\\
&+\int_0^{1/2}dx\left[\frac{(t-2)(s+1-r)}{[1-tx(1-x)]\sqrt{R_t}}\ln\frac{s+1-r+\sqrt{R_t}}{s+1-r-\sqrt{R_t}}\right.\\
&\left.+\frac{(t-2r)(s-1+r)}{[r-tx(1-x)]\sqrt{R_t}}\ln\frac{s-1+r+\sqrt{R_t}}{s-1+r-\sqrt{R_t}}\right]\\
&+\int_0^1 dx\left[\frac{(s-1-r)[s+(1-r)(1-2x)]}{(1-2x)[sx(1-x)+(1-2x)(1-x-rx)]\sqrt{P}}\right.\\
&\times\ln\frac{s+(1-2x)(1-r+\sqrt{P})}{s+(1-2x)(1-r-\sqrt{P})}\\
&\left.+\frac{(u-1-r)[s+(1-r)(1-2x)]}{[1+(r-1)x-ux(1-x)]\sqrt{R_u}}\ln\frac{s+(1-r)(1-2x)+\sqrt{R_u}}{s+(1-r)(1-2x)-\sqrt{R_u}}\right]\Bigg\}, \qquad (20)
\end{aligned}
$$

where we have introduced the polynomials: $P=s^2-2s(1+r)+(1-r)^2$, $R_t=P+4stx(1-x)$, $R_u=P+4x(1-x)[su-(1-r)^2]$. We note that the terms beyond those proportional to $\ln(m_e/2\lambda)-\xi_{IR}$ are specific for the evaluation of the soft photon correction factor $\delta_{\rm soft}$ in the center-of-mass frame with λ an infrared cut-off therein. As it is written in eq.(20), $\delta_{\rm soft}^{\rm (cm)}$ refers to an (idealized) experimental situation where all undetected soft photon radiation fills a small sphere of radius λ in the center-of-mass frame. In a real experiment the momentum space region of undetected photons can be of different (non-isotropic) shape with no sharp boundaries due to detector efficiencies etc. Such additional experiment-specific radiative corrections can be accounted for and calculated by integrating the fivefold differential cross section for $e^-\pi^-\to e^-\pi^-\gamma$ over the appropriate region in phase space. By construction this region excludes the infrared singular domain $|\vec{l}|<\lambda$ and thus leads to a finite result. The treatment of hard photon bremsstrahlung [8] may also be important for comparison with a real experiment.

2.3 Numerical results

We are now in the position to present some numerical results for the radiative corrections to electron-pion scattering $e^-\pi^-\to e^-\pi^-$. The complete (infrared-finite) radiative correction factor is $\delta_{\rm soft}^{\rm (cm)}$ written in eq.(20) plus the sum of all interference terms (see eq.(2)) divided by the Born term $A\otimes A/t^2$. We refer to the center-of-mass kinematics where $t=(\cos\theta_{\rm cm}-1)P/2s$ (and $u=2+2r-s-t$), with $\theta_{\rm cm}$ the scattering angle and $P=s^2-2s(1+r)+(1-r)^2$. Fig. 5 shows in percent the radiative corrections arising from loops alone (discarding the ξ_{IR} terms) at five selected center-of-mass energies $\sqrt{s}\,m_\pi=(1,1,\,1.6,\,2.1,\,2.6,\,3.1)m_\pi$ as a function of $\cos\theta_{\rm cm}$. One notices sizeable negative radiative corrections with values up to about -11.5%. With increasing $\sqrt{s}$ the curves become gradually more symmetric under forward and backward directions, $\theta_{\rm cm}\to 180^\circ-\theta_{\rm cm}$. At the highest selected center-of-mass energy $\sqrt{s}\,m_\pi=3.1m_\pi$ the maximal squared momentum transfer is $-t_{\rm max}m_\pi^2=0.15\,{\rm GeV}^2$. This corresponds to the region within which accurate data for pion-electron scattering [2] are presently available [10].

[2]For elastic pion-electron scattering the squared momentum transfer is given by $-tm_\pi^2=2m_e(p_3^0-m_e)$ with p_3^0 the electron recoil energy. Since m_e occurs as a determining factor, pion beams with energies in the

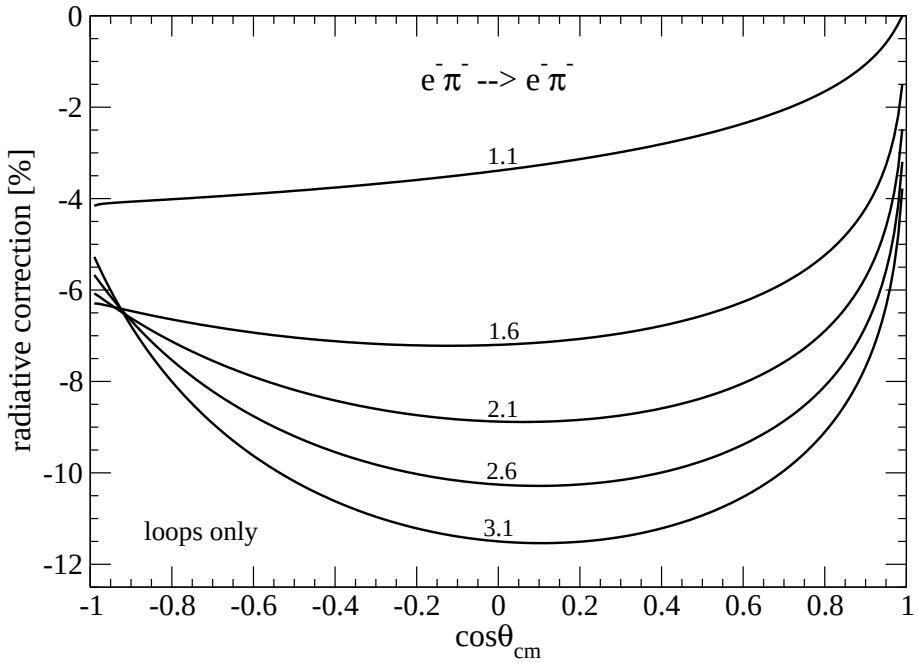

Figure 5: Radiative corrections to electron-pion scattering $e^-\pi^- \to e^-\pi^-$ arising from loops. The numbers $(1.1, 1.6, 2.1, 2.6, 3.1)$ on the curves correspond to the total center-of-mass energy $\sqrt{s}\, m_\pi$ in units of m_π.

Let us look also at individual contributions to the radiative corrections. For example, at $\sqrt{s} = 3$ and $\theta_{\rm cm} = 120^\circ$ one has $[(-14.90 - 2.51) + (1.74 + 0.16 + 0.016) + 5.51]\% = -9.99\%$, where the numbers in brackets stem from photonic vertex correction, vacuum polarization and two-photon-exchange, in the order presented in subsection 2.1. The contribution from the two-photon exchange triangle diagram III is in fact tiny: -0.0003%. This observation supports the approach of ref.[7] that the finite size of the pion can be ignored for this (extremely small) contribution. Evidently, the radiative corrections to electron-pion scattering $e^-\pi^- \to e^-\pi^-$ are dominated by the electronic vertex correction due to the leading squared logarithm in the asymptotic behavior of the Dirac form factor $F_1(t)^{\gamma-\rm loop} \simeq -(\alpha/4\pi)\ln^2(-tr^{-1})$. Next in importance follows the two-photon exchange in form of the box diagrams IV and V. In principle the contribution $\Pi_\pi \otimes A$ from pionic vacuum polarization should replaced by that of hadronic vacuum polarization $(A \otimes A)\Pi_{\rm had}(t)/t$. However, for the small momentum transfers $\sqrt{-t} m_\pi < 0.4\,\mathrm{GeV}$ considered here, the corresponding (hadronic) effect is very small and reasonably well approximated by the vacuum polarization due to a pointlike pion. The empirical vacuum polarization function with its leptonic and hadronic contributions is shown in Fig. 82 of ref.[9].

Fig. 6 shows the radiative corrections to electron-pion scattering $e^-\pi^- \to e^-\pi^-$ with inclusion of the soft photon bremsstrahlung effects. For the sake of having a concrete case we have set the infrared cutoff to the value $\lambda = \sqrt{s}\, m_\pi/200$, thus modelling an (idealized) experimental situation where the electron and pion energies can be resolved within 1% accuracy. One observes that the soft photon bremsstrahlung increases moderately the (negative) radiative corrections to electron-pion scattering. At $\sqrt{s} = 3$ and $\theta_{\rm cm} = 120^\circ$ one has a soft photon correction of $(10.50 - 17.41)\% = -6.91\%$, where the first and second number refer to the "universal" part proportional to $\ln(m_e/2\lambda)$ and to the remaining terms in eq.(20) specific for imposing an infrared cutoff via $|\vec{l}\,| < \lambda$ the center-of-mass frame. It is clear that the radiative

few TeV range would be needed in order to reach a (modest) momentum transfer of $\sqrt{-t} m_\pi \simeq 1\,\mathrm{GeV}$.

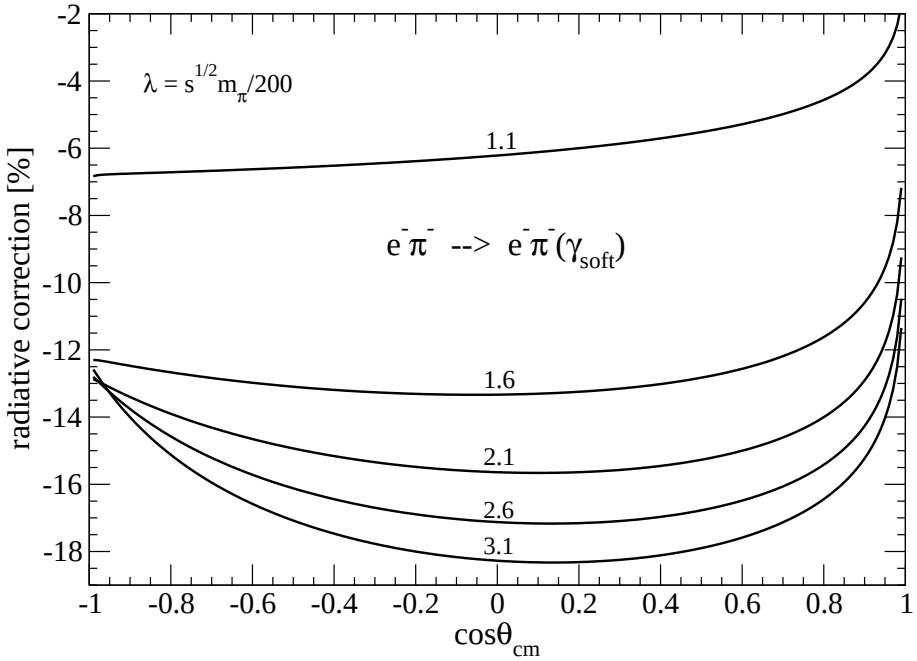

Figure 6: Radiative corrections to electron-pion scattering $e^-\pi^- \to e^-\pi^-$ including soft photon bremsstrahlung. The numbers $(1.1, 1.6, 2.1, 2.6, 3.1)$ on the curves correspond to the total center-of-mass energy $\sqrt{s}\, m_\pi$ in units of m_π. The infrared cutoff has been set to $\lambda = \sqrt{s}\, m_\pi/200$.

corrections due to the inelastic bremsstrahlung process $e^-\pi^- \to e^-\pi^-\gamma$ depend crucially on the particular experimental conditions (i.e. cuts on energies and angles).

3 Radiative corrections to pion-pair production

In this section we discuss the radiative corrections to pion-pair production in e^-e^+ annihilation. The process $e^-e^+ \to \pi^+\pi^-$ is obtained from elastic electron-pion scattering $e^-\pi^- \to e^-\pi^-$ via the crossing transformation $s \leftrightarrow t$. We prefer to keep the original meaning of the Mandelstam variables and thus denote by $\sqrt{t}\, m_\pi$ the total center-of-mass energy of the reaction $e^-e^+ \to \pi^+\pi^-$. The cosine of the scattering angle $y = \cos\theta_{\rm cm}$ is involved in the (uncrossed) variable $u = 1 + r + (y\sqrt{t-4}\sqrt{t-4r} - t)/2$ and $s = 2 + 2r - t - u$ receives the same form with $y \to -y$. The relevant angular average $\frac{1}{2}\int_{-1}^{1} dy \ldots$ of the tree amplitude $A \otimes A$ comes out as $(4-t)(t+2r)/6$. With an additional factor $-1/2$ due to averaging over positron spin-states the total cross section for pion-pair production has the following well-known form:

$$\sigma_{\rm tot}(t) = \frac{\pi\alpha^2}{3m_\pi^2 t^3}\frac{(t-4)^{3/2}}{\sqrt{t-4r}}(t+2r)\,. \tag{21}$$

The analytical expressions for the loop contributions to pion-pair production $e^-e^+ \to \pi^+\pi^-$ can be directly taken over from subsection 2.1. The angular integration $2\pi\int_{-1}^{1} dy$ involved in the total cross section eliminates all terms which are odd under the permutation of variables $s \leftrightarrow u$. These are precisely the two-photon exchange contributions (III+IV+V)$\otimes A$ given in eqs.(13,15,17). The virtual radiative corrections (of order α) to the total cross section $\sigma_{\rm tot}(e^-e^+ \to \pi^+\pi^-)$ are therefore completely determined by the photonic vertex corrections I$\otimes A$ and the vacuum polarizations II$\otimes A$. By making use of the angular average $(4-t)(t+2r)/6$ of $A \otimes A$ they can be directly read off from eqs.(5,10-12) with their explicit t-dependence.

The soft photon correction factor for pion-pair production $e^-e^+ \to \pi^+\pi^-$ is a modified version of eq.(19) due to sign-changes of charges. When evaluated for the center-of-mass kinematics under consideration it reads [11]:

$$\begin{aligned}
\delta_{\rm soft}^{\rm (cm)} &= \frac{\alpha}{\pi}\Bigg\{4\bigg[1+\frac{2-t}{\sqrt{t}}\,L(t-4)+\frac{2r-t}{\sqrt{tr}}\,L\Big(\frac{t}{r}-4\Big)\bigg]\Big(\ln\frac{m_e}{2\lambda}-\xi_{IR}\Big) \\
&\quad +2\sqrt{\frac{t}{r}}\,L\Big(\frac{t}{r}-4\Big)+2\sqrt{t}\,L(t-4) \\
&\quad +\int_0^{1/2}dx\bigg[\frac{\sqrt{t}(2-t)(t-4)^{-1/2}}{(1-2x)[1+(t-4)x(1-x)]}\ln\frac{\sqrt{t}+(1-2x)\sqrt{t-4}}{\sqrt{t}-(1-2x)\sqrt{t-4}} \\
&\quad +\frac{\sqrt{t}(2r-t)(t-4r)^{-1/2}}{(1-2x)[r+(t-4r)x(1-x)]}\ln\frac{\sqrt{t}+(1-2x)\sqrt{t-4r}}{\sqrt{t}-(1-2x)\sqrt{t-4r}}\bigg] \\
&\quad +\text{ terms odd under } (s\leftrightarrow u)\Bigg\}, \qquad (22)
\end{aligned}$$

with the function $L(x)$ defined in eq.(6). The terms odd under $s \leftrightarrow u$ need not to be specified. After multiplication with the even Born term $A \otimes A$ and subsequent angular integration $2\pi \int_{-1}^{1} dy$ they drop out of the radiative corrections to $\sigma_{\rm tot}(t)$.

The dashed line in Fig. 7 shows the radiative corrections to the total cross section for pion-pair production $e^-e^+ \to \pi^+\pi^-$ arising from loops alone (discarding the ξ_{IR} terms) . One observes sizeable (negative) radiative corrections which increase with center-off-mass energy $\sqrt{t}\,m_\pi$. For example, at $\sqrt{t} = 4$ one has $[(-16.80 - 2.70) + (1.91 + 0.22)]\% = -17.37\%$, where the numbers in brackets correspond to photonic vertex correction and leptonic vacuum polarization, in the order presented in subsection 2.1. The photon-loop correction to the photon-electron vertex is again the dominant effect. Next in importance follows the same type of correction to the photon-pion vertex. The dashed line in Fig. 8 shows the radiative corrections to the total cross section for pion-pair production $e^-e^+ \to \pi^+\pi^-$ with inclusion of soft photon bremsstrahlung effects. For the sake of having a concrete case we have set the infrared cutoff to the value $\lambda = \sqrt{t}\,m_\pi/200$. One observes a further increase of the negative radiative corrections, but now their rise with the center-of-mass energy $\sqrt{t}\,m_\pi$ has significantly slowed down. Note that we have dropped here the contribution $\mathrm{II}_\pi \otimes A$ from pionic vacuum polarization since it does not even in an approximate way represent the effects from hadronic vacuum polarization in the energy region $\sqrt{t}m_\pi < 1\,\mathrm{GeV}$ of interest. As can be seen from Fig. 82 in ref.[9] the empirical hadronic vacuum polarization function develops pronounced oscillations with sharp spikes in that energy range. Radiative corrections to the differential cross section for $e^-e^+ \to \pi^+\pi^-$ at yet higher orders in α have been studied by Hoefer et al. in ref.[12].

3.1 Inclusion of pion structure

With good reason one may object that treating the pion as a structureless spin-0 particle in a calculation of the radiative corrections to $e^-e^+ \to \pi^+\pi^-$ for energies up to $\sqrt{t}\,m_\pi \simeq 1\,\mathrm{GeV}$ is rather unrealistic. In the $\rho(770)$-resonance region the empirical charge form factor of the pion leads to an enhancement of the total cross section by a factor of up to 45. One is therefore obliged to include the structure (finite size) of the pion also in the calculation of the radiative corrections. As motivated by the vector meson dominance model, we introduce at each photon-pion vertex a "bare" pion charge form factor of monopole type: $F_\pi(-q^2) = (1 - q^2/m_\rho^2)^{-1}$, with $m_\rho = 770\,\mathrm{MeV}$ the (neutral) ρ-meson mass. Here, q is the photon four-momentum and

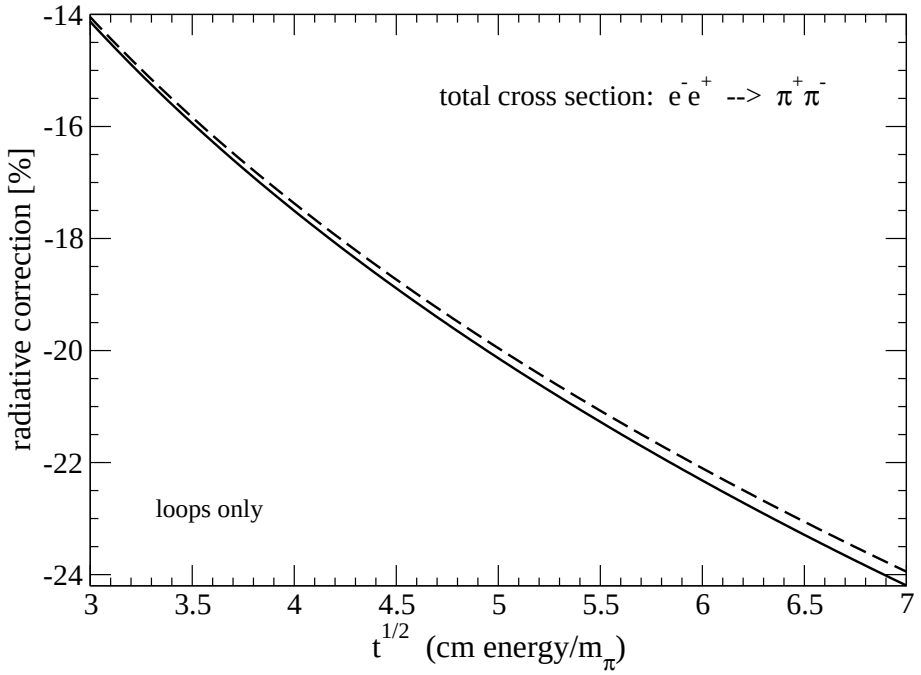

Figure 7: Radiative corrections to the total cross section for pion-pair production $e^-e^+ \to \pi^+\pi^-$ arising from loops. The dashed line corresponds to a structureless pion. The full line includes pion-structure through a vector meson dominance form factor. Hadronic vacuum polarization [9] is not considered explicitly.

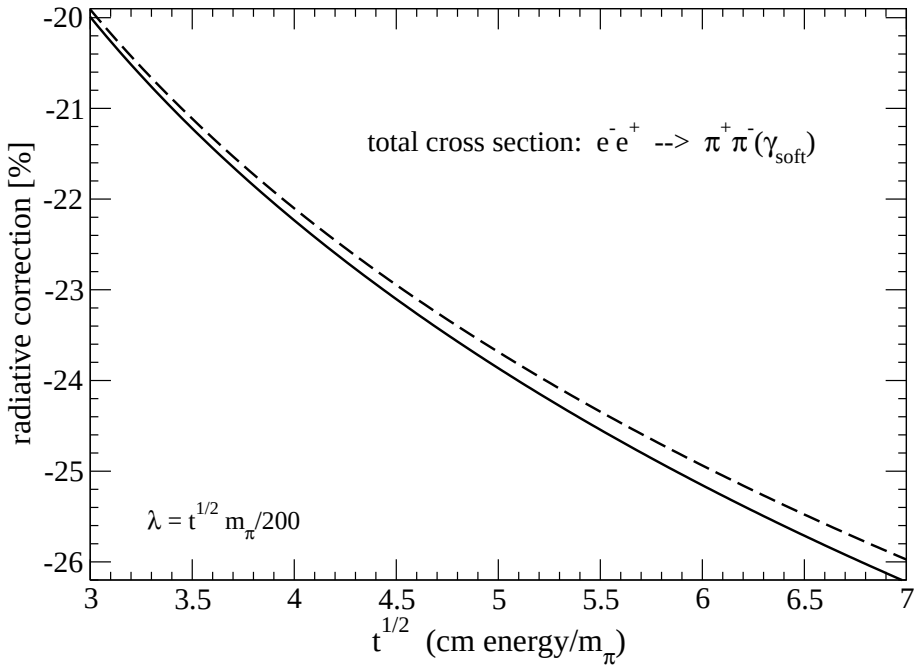

Figure 8: Radiative corrections to the total cross section for pion-pair production $e^-e^+ \to \pi^+\pi^-$ with inclusion of soft photon bremsstrahlung. The dashed line corresponds to a structureless pion. The full line includes pion-structure through a vector meson dominance form factor. Hadronic vacuum polarization [9] is not considered explicitly.

we apply the same form of $F_\pi(-q^2)$ irrespective of whether the in- and out-going pions are on or off their mass-shell. A first success of such an (admittedly crude) approach is the pion electromagnetic selfenergy. When evaluated with a squared monopole form factor inserted the one-photon loop selfenergy diagrams lead to the following expression for the mass difference between the charged and neutral pion:

$$\Delta_\pi = \frac{\alpha}{2\pi} m_\rho \Big[z + 2z^3 \ln 2z - (2z^2+1)\sqrt{z^2-1}\ln(z+\sqrt{z^2-1}) \Big] , \tag{23}$$

with the ratio $z = m_\rho/2m_{\pi^0} = 2.852$. The value $\Delta_\pi = 4.31\,\mathrm{MeV}$ resulting from this simple model is remarkably close to the experimental pion mass difference $\Delta_\pi^{(\mathrm{exp})} = 4.59\,\mathrm{MeV}$. The small remainder is (generally) attributed to an isospin-breaking effect quadratic in the up- and down-quark mass difference.

We apply now the monopole form factor $F_\pi(-q^2)$ consistently to all photon-pion vertices of the diagrams in Fig. 1,2,3 and mark these modified diagrams by a prime. The modified Born term reads:

$$A' \otimes A' = \frac{b^2}{(b-t)^2} \, (A \otimes A) \, , \tag{24}$$

with $b = (m_\rho/m_\pi)^2 = 30.44$, and similarly one gets for diagram I'_e with electronic vertex correction:

$$\mathrm{I}'_e \otimes A' = \frac{b^2}{(b-t)^2} \, (\mathrm{I}_e \otimes A) \, . \tag{25}$$

For the (pionic) vertex correction diagrams I'_π we exploit identity:

$$\frac{m_\rho^4}{(-l^2)(m_\rho^2-l^2)^2} = \frac{1}{-l^2} + \Big(m_\rho^2 \frac{\partial}{\partial m_\rho^2} - 1 \Big) \frac{1}{m_\rho^2 - l^2} \, , \tag{26}$$

which shows that the photon-loop with a squared monopole form factor inserted is equal to an ordinary photon-loop plus a term which can be calculated from a massive vector-meson loop by differentiation with respect to its mass. It is most convenient to calculate directly the imaginary part of the (ordinary) vector-meson loop via the Cutkosky cutting rule and to apply (after the mass-differentiation) a once-subtracted dispersion relation.[3] Putting all the pieces together one obtains the following modified interference term:

$$\begin{aligned} \mathrm{I}'_\pi \otimes A' \;\; = \;\; & \frac{b^2}{(b-t)^2} \, (\mathrm{I}_\pi \otimes A) + \frac{\alpha}{2\pi} (A' \otimes A') \int_4^\infty dx \frac{1}{\sqrt{x^2-4x}\,(x-t)} \\ & \times \Big[1 - \frac{2+b}{x} - \frac{b}{2(x-4+b)} + \Big(\frac{2}{x} - 1 + \frac{b^2}{x^2-4x} \Big) \ln \frac{x-4+b}{b} \Big] . \end{aligned} \tag{27}$$

For $t > 4$, the real part of the spectral integral $\int_4^\infty dx/(x-t) \ldots$ is given by its principal value. Finally, there are the modified contributions from electronic and muonic vacuum polarization:

$$\mathrm{II}'_{e,\mu} \otimes A' = \frac{b^2}{(b-t)^2} \, (\mathrm{II}_{e,\mu} \otimes A) \, , \tag{28}$$

as well as from hadronic vacuum polarization:

$$\mathrm{II}'_{\mathrm{had}} \otimes A' = \frac{A' \otimes A'}{t} \Pi_{\mathrm{had}}(t) \, , \qquad \mathrm{Re}\,\Pi_{\mathrm{had}}(t) = \frac{t}{4\pi^2\alpha} \int_{4m_\pi^2}^\infty ds' \frac{\sigma^0_{\mathrm{had}}(s')}{t - s' m_\pi^{-2}} \, , \tag{29}$$

[3] We have verified that the normalization condition $G_\pi(0)^{\gamma-\mathrm{loop}} = 0$ for the photon-loop induced pion form factor is preserved if the vertices include a monopole form factor. In addition to the diagrams I'_π in Fig. 2 there is also a b-dependent pion wavefunction renormalization factor, $Z_2^{(\pi)} - 1 = (\alpha/4\pi)\big\{ 4\xi_{IR} - 2\ln r + b - 2 + (2 - b^2/2)\ln b + \sqrt{b/(b-4)}\,(b^2-2b-2)\ln[(\sqrt{b}+\sqrt{b-4})/2] \big\}$, which contributes to the zero-sum.

with $\sigma^0_{\rm had}(s')$ the (undressed) cross section for electron-positron annihilation into hadrons [9]. The two-photon exchange contribution (III′ + IV′ + V′)⊗A′ remains of course odd under $s \leftrightarrow u$ and thus drops out of the radiative corrections to the total cross section $\sigma_{\rm tot}(e^-e^+ \to \pi^+\pi^-)$. Note that the assumption of a monopole for the pion charge form factor plays only a role for the second term in eq.(27). After dividing by the modified Born term $A' \otimes A'$ the actual functional form of $|F_\pi(-tm_\pi^2)|^2$ drops out in the radiative corrections of interest. Accurate empirical parameterization of the pion charge form factor $F_\pi(-q^2)$ which include the finite width of the (neutral) $\rho(770)$-meson and the (isospin-breaking) ρ^0-ω interference can be found in appendix C of ref.[12].

The full line in Fig. 7 shows the radiative corrections to $\sigma_{\rm tot}(e^-e^+ \to \pi^+\pi^-)$ arising from loops with inclusion of the pion-structure. The individual contributions to the radiative correction factor at $\sqrt{t} = 4$ are now: $[(-16.80 - 2.83) + (1.91 + 0.22)]\% = -17.50\%$. By comparison with the dashed line in Fig. 7 one sees that the effects due to the pion-structure are very small. The essentially new principal-value integral term in eq.(27) arising from the photon-loop with monopole-type vertex functions amounts at $\sqrt{t} = 4, 5.5, 7$ to radiative corrections of $(-0.13, -0.20, -0.25)\%$, respectively. The full line in Fig. 8 shows the analogous results with inclusion of the soft photon bremsstrahlung effects. The latter are given by eq.(22) in unchanged form since for real photon emission ($q^2 = 0$) the form factor effect vanishes (according to our treatment which does not make a distinction between on- and off-shell pions).

Let us exhibit separately the correction induced by the finite size of the pion on the photon-loop form factor $G_\pi(t)^{\gamma-\rm loop}$ of the pion:

$$\begin{aligned}\delta G_\pi(t)^{\gamma-\rm loop} &= \frac{\alpha t}{2\pi}\int_4^\infty \frac{dx}{x-t-i0}\,\frac{1}{\sqrt{x^2-4x}}\Big\{1 - \frac{b}{2(x-4+b)} \\ &\quad -\frac{2+b}{x} + \Big(\frac{2}{x} - 1 + \frac{b^2}{x^2-4x}\Big)\ln\frac{x-4+b}{b}\Big\}. \end{aligned} \tag{30}$$

The full and dashed line in Fig. 9 show the real and imaginary part of this quantity in the interval $-50 < t < 50$. One observes very small values which range between 1.1 permille and -1.4 permille. At the branch point $t = 4$ this finite size correction reads:

$$\delta G_\pi(4)^{\gamma-\rm loop} = \frac{\alpha}{6\pi}\Big\{3 + 2b - b^2\ln b + \frac{2}{\sqrt{b(b-4)}}(b^3 - 2b^2 - 2b - 6)\ln\frac{\sqrt{b} + \sqrt{b-4}}{2}\Big\}, \tag{31}$$

and the slope at $t = 0$ is given by:

$$\begin{aligned}\delta G'_\pi(0)^{\gamma-\rm loop} &= \frac{\alpha}{24\pi}\Big\{(4 + b^2)\ln b - 3 - 2b - \frac{20}{b-4} + \frac{2\sqrt{b}}{(b-4)^{3/2}} \\ &\quad \times(6b^2 - b^3 - 10b + 18)\ln\frac{\sqrt{b} + \sqrt{b-4}}{2}\Big\}, \end{aligned} \tag{32}$$

with $b = (m_\rho/m_\pi)^2 = 30.44$. It remains to be seen how much the finite size correction $\delta G_\pi(t)^{\gamma-\rm loop}$ changes if an improved parameterization of the half off-shell pion-photon vertex function is used. The electromagnetic selfenergy Δ_π given in eq.(23) suggests that the present treatment could be fairly reasonable.

Finally, we note that the radiative corrections to pion- and kaon-pair production in e^-e^+ collisions for energies below 2 GeV have also been calculated by Arbuzov et al. in ref.[13]. In that work the differential cross section $d\sigma/d\Omega_{\rm cm}$ of the reaction has been considered and the radiative corrections have been approximated by their leading logarithms in the electron mass

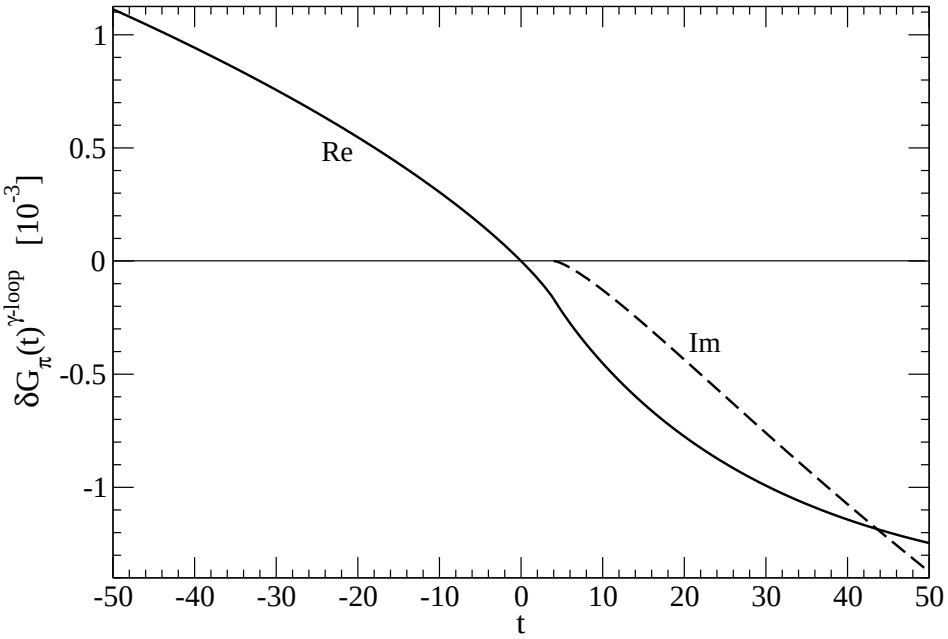

Figure 9: Correction to the photon-loop form factor of the pion induces by the finite size of the pion. The calculation is based on a pion charge from factor of monopole type.

m_e. The structure (i.e. finite size) of the mesons has however not been taken into account and the accuracy of their calculation [13] has been estimated to about 0.2%. This numerical estimate is remarkably consistent with our present finding for the size of the additional radiative corrections induced by the pion-structure.

References

[1] L.C. Maximon, *Rev. Mod. Phys.* **41**, 193 (1969).

[2] L.W. Mo and Y.S. Tsai, *Rev. Mod. Phys.* **41**, 205 (1969).

[3] P.A.M. Guichon and M. Vanderhaeghen, *Phys. Rev. Lett.* **91**, 142303 (2003).

[4] P.G. Blunden, W. Melnitchouk and J.A. Tjon, *Phys. Rev. Lett.* **91**, 142304 (2003).

[5] P.G. Blunden, W. Melnitchouk and J.A. Tjon, *Phys. Rev.* **C72**, 034612 (2005).

[6] C.E. Carlson and M. Vanderhaeghen, *Annu. Rev. Nucl. Part. Sci.* **57**, 171 (2007).

[7] P.G. Blunden, W. Melnitchouk and J.A. Tjon, *Phys. Rev.* **C81**, 018202 (2010); and refs. therein.

[8] J. Kahane, *Phys. Rev.* **135B**, 975 (1964).

[9] Working Group on Radiative Corrections and Monto Carlo Generators for Low Energies: S. Actis et al., *Eur. Phys. J.* **C66**, 585 (2010); and refs. therein.

[10] NA7 Collaboration: S.R. Amendolia et al., *Phys. Lett.* **B146**, 116 (1984); *Nucl. Phys.* **B277**, 168 (1988).

[11] N. Kaiser, *J. Phys. G: Nucl. Part. Phys.*, 115005 (2010).

[12] A. Hoefer, J. Gluza, F. Jegerlehner, *Eur. Phys. J.* **C24**, 51 (2002); and refs. therein.

[13] A.B. Arbuzov et al., *JHEP* **9710**, 006 (1997); hep-ph/9703456.